

# Pyramid diffraction in parity-time-symmetric optical lattices

Sean Nixon and Jianke Yang

*Department of Mathematics and Statistics, University of Vermont, Burlington, VT 05401, USA*

Nonlinear dynamics of wave packets in two-dimensional parity-time-symmetric optical lattices near the phase-transition point are analytically studied. A novel fourth-order equation is derived for the envelope of these wave packets. A pyramid diffraction pattern is demonstrated in both the linear and nonlinear regimes. Blow-up is also possible in the nonlinear regime for both focusing and defocusing nonlinearities.

Parity-time ( $\mathcal{PT}$ )-symmetric wave systems have the unintuitive property that their linear spectrum can be completely real even though they contain gain and loss [1]. In spatial optics,  $\mathcal{PT}$ -symmetric systems can be realized by employing symmetric index guiding and an antisymmetric gain/loss profile [2–5]. In temporal optics,  $\mathcal{PT}$ -symmetric systems can be obtained as well [6–8]. So far, a number of novel phenomena in optical  $\mathcal{PT}$  systems have been reported, including phase transition, non-reciprocal Bloch oscillation, unidirectional propagation, distinct pattern of diffraction, formation of solitons and breathers, wave blow-up, and so on [4–14].

In this Letter, we analytically study nonlinear dynamics of wave packets in two-dimensional  $\mathcal{PT}$ -symmetric optical lattices near the phase-transition point (where diffraction surfaces of Bloch bands cross like the intersection of four planes). Near these intersections we show that the evolution of wave packets is governed by a novel fourth-order equation. Based on this envelope equation, we predict a pyramid (i.e., expanding square) diffraction pattern in both linear and nonlinear regimes. Further, in the nonlinear regime blow-up can occur for both focusing and defocusing nonlinearities. These predictions are verified in the full equation as well.

The model for nonlinear propagation of light beams in  $\mathcal{PT}$ -symmetric optical lattices is taken as

$$i\Psi_z + \nabla^2\Psi + V(x, y)\Psi + \sigma|\Psi|^2\Psi = 0, \quad (1)$$

where  $z$  is the propagation direction,  $(x, y)$  is the transverse plane,  $\nabla^2 = \partial_x^2 + \partial_y^2$ , and  $\sigma = \pm 1$  is the sign of nonlinearity. The  $\mathcal{PT}$ -symmetric potential  $V(x, y)$  is taken as  $V(x, y) = \tilde{V}(x) + \tilde{V}(y)$ , where

$$\tilde{V}(x) = V_0^2 [\cos(2x) + iW_0 \sin(2x)], \quad (2)$$

$V_0^2$  is the potential depth and  $W_0$  is the relative gain/loss strength.

We begin by considering the linear diffraction relation of Eq. (1) at the phase-transition point  $W_0 = 1$  [9, 13]. In this case, the linear equation of (1) can be solved exactly [13]. The diffraction relation is  $\mu = (k_x + 2m_1)^2 + (k_y + 2m_2)^2$ , where  $(k_x, k_y)$  are Bloch wavenumbers in the first Brillouin zone  $-1 \leq k_x, k_y \leq 1$ , and  $(m_1, m_2)$  are any pair of nonnegative integers. The most complex degeneracies occur at points  $k_x = 0, \pm 1$  and  $k_y = 0, \pm 1$ , where the diffraction surface intersects itself four-fold as illustrated in Fig. 1. If a carrier Bloch

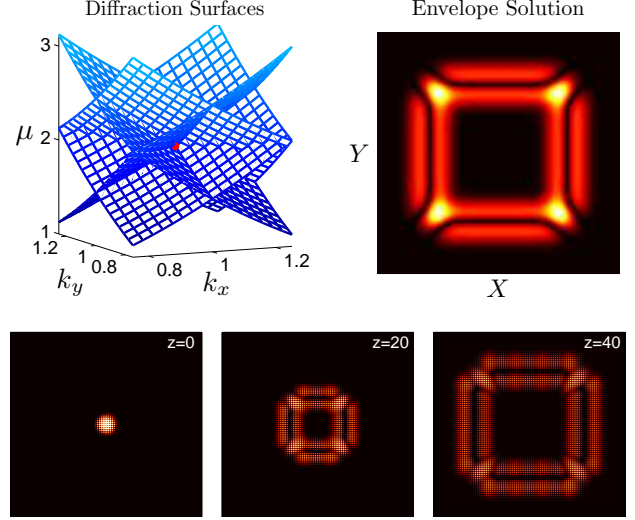


FIG. 1: (Upper left) Diffraction relation near the intersection point  $(k_x, k_y, \mu) = (1, 1, 2)$  (marked by a red dot). (Upper right) Linear-diffraction pattern of an initial Gaussian envelope at phase transition in the envelope equation (11). (Lower row) Linear diffraction of an initial Gaussian wave packet at phase transition in the full equation (1).

wave is chosen at one of these degeneracies, then the envelope of the resulting wave packet exhibits novel behavior which we elucidate below.

To analyze the structure of these degeneracies we exploit the fact that the potential  $V(x, y)$  is separable. Posed as an eigenvalue problem for  $\Psi = \phi(x, y)e^{-i\mu z}$  in the linear equation of (1), we get  $L\phi = -\mu\phi$ , where  $L = L^{(x)} + L^{(y)}$ ,  $L^{(x)} \equiv \partial_x^2 + \tilde{V}_0(x)$ , and  $\tilde{V}_0(x)$  is the  $\mathcal{PT}$  lattice (2) at the phase-transition point  $W_0 = 1$ . At four-fold intersection points, the eigenvalues are  $\mu = n_1^2 + n_2^2$ , where  $(n_1, n_2)$  are any pair of positive integers. The operator  $L^{(x)}$  ( $L^{(y)}$ ) has eigenvalues  $n_1^2$  ( $n_2^2$ ) with geometric multiplicity 1 and algebraic multiplicity 2 [14]. Let  $\phi^{e1}(x)$  ( $\phi^{e2}(y)$ ) be the eigenfunction and  $\phi^{g1}(x)$  ( $\phi^{g2}(y)$ ) the associated generalized eigenfunction. Then

$$\phi^{e1}(x) = \tilde{I}_{n_1}(V_0 e^{ix}), \quad \phi^{e2}(y) = \tilde{I}_{n_2}(V_0 e^{iy}), \quad (3)$$

where  $\tilde{I}_n(V_0 e^{ix})$  is the modified Bessel function  $I_n(V_0 e^{ix})$  normalized to have unit peak amplitude, and  $(L^{(x)} + n_1^2)\phi^{g1} = \phi^{e1}$ ,  $(L^{(y)} + n_2^2)\phi^{g2} = \phi^{e2}$ . Since  $L = L^{(x)} + L^{(y)}$ ,

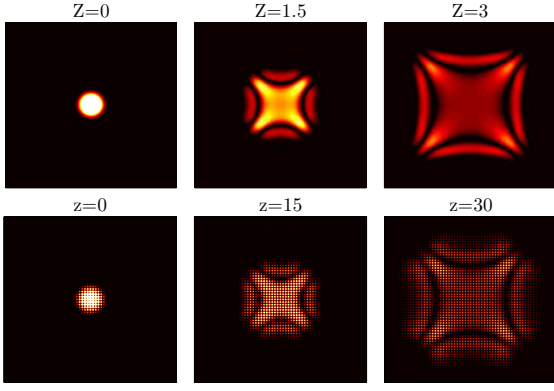


FIG. 2: Pyramid diffraction of a Gaussian wavepacket in the linear equation below phase transition. Upper row: diffraction in the envelope equation (11); lower row: diffraction in the full equation (1).

we see that  $L$  has two eigenfunctions

$$\phi^{01}(x, y) = \phi^{e_1}(x)\phi^{e_2}(y), \quad (4a)$$

$$\phi^{02}(x, y) = \phi^{e_1}(x)\phi^{g_2}(y) - \phi^{g_1}(x)\phi^{e_2}(y). \quad (4b)$$

In addition, the first eigenfunction  $\phi^{01}$  has two generalized eigenfunctions

$$\phi^{11}(x, y) = [\phi^{e_1}(x)\phi^{g_2}(y) + \phi^{g_1}(x)\phi^{e_2}(y)]/2, \quad (5a)$$

$$\phi^{21}(x, y) = \phi^{g_1}(x)\phi^{g_2}(y), \quad (5b)$$

where  $(L + \mu)\phi^{11} = \phi^{01}$ , and  $(L + \mu)\phi^{21} = \phi^{11}$ .

We now study the nonlinear dynamics of wave packets near these intersections. For simplicity, we will conduct the analysis at the lowest intersection point,  $\mu = 2$ . But similar results can be obtained for any intersection point.

The perturbation expansion for the wave packet near the intersection  $\mu = 2$  is

$$\Psi = \epsilon^{\frac{3}{2}}\psi e^{-i\mu t}, \quad \psi = \psi_0 + \epsilon\psi_1 + \dots, \quad (6)$$

where  $\psi_0 = A(X, Y, Z)\phi^{01}(x, y)$  is the leading-order wave packet for the Bloch mode  $\phi^{01}$  at the intersection point  $(k_x, k_y, \mu) = (1, 1, 2)$ ,  $(X, Y, Z) = (\epsilon x, \epsilon y, \epsilon z)$  are slow spatial variables, and  $0 < \epsilon \ll 1$ . Near the phase-transition point,  $W_0$  can be expressed as  $W_0 = 1 - \eta\epsilon^2/V_0^2$ , where  $\eta$  measures the deviation from phase-transition. After introducing the slow variables into equation (1), the new equation for  $\psi$  is

$$(L + \mu)\psi = -i\epsilon\psi_Z - 2\epsilon(\psi_{xX} + \psi_{yY}) - \epsilon^2(\partial_X^2 + \partial_Y^2)\psi + i\eta\epsilon^2[\sin(2x) + \sin(2y)]\psi - \epsilon^3\sigma|\psi|^2\psi. \quad (7)$$

We proceed by inserting expansion (6) into equation (7) and solving for  $\psi_n$  at each order. Each  $\psi_n$  satisfies a linear inhomogeneous equation, with the homogeneous operator being  $L + \mu$ . In order for it to be solvable, the Fredholm conditions need to be satisfied, i.e., the

inhomogeneous term must be orthogonal to the kernels  $\phi^{01*}$  and  $\phi^{02*}$  of the adjoint operator  $L^* + \mu$ . Here  $*$  stands for complex conjugation.

At  $O(\epsilon)$  the solvability conditions for  $\psi_1$  are automatically satisfied, and thus we can solve  $\psi_1$  as

$$\psi_1 = -iA_T\phi^{11} - 2A_X\phi^a - 2A_Y\phi^b + B\phi^{02}, \quad (8)$$

where  $B(X, Y, Z)$  is the envelope of the second eigenfunction  $\phi^{02}$ ,  $(L + \mu)\phi^a = \phi_x^{01}$ ,  $(L + \mu)\phi^b = \phi_y^{01}$ , and  $\phi^a, \phi^b$  are assumed to be orthogonal to  $\phi^{01}$  and  $\phi^{02}$ .

Now we proceed to the  $\psi_2$  equation at  $O(\epsilon^2)$ . The orthogonality condition with  $\phi^{01*}$  is automatically satisfied, and the orthogonality condition with  $\phi^{02*}$  gives

$$iB_Z = A_{ZX} - A_{ZY} + 2A_{XX} - 2A_{YY}, \quad (9)$$

which defines the connection between envelopes  $A$  and  $B$  of the two eigenmodes at the Bloch-surface intersection. Under this relation, the  $\psi_2$  equation can be solved.

Finally we proceed to the  $\psi_3$  equation at  $O(\epsilon^3)$ . The orthogonality condition with  $\phi^{01*}$  gives

$$\partial_Z^3 A - 8(\partial_X^2 + \partial_Y^2)\partial_Z A - 8(\partial_X^2 - \partial_Y^2)(\partial_X - \partial_Y)A + 8(\partial_X^2 - \partial_Y^2)(iB) + \alpha\partial_Z A + i\tilde{\sigma}|A|^2 A = 0, \quad (10)$$

where

$$\alpha = 2V_0^2\eta, \quad \tilde{\sigma} = -i\sigma \frac{\int_0^{2\pi} \int_0^{2\pi} |\phi^{01}|^2 \phi^{01} \phi^{21} dx dy}{\int_0^{2\pi} \int_0^{2\pi} \phi^{01} \phi^{21} dx dy}.$$

This equation, combined with equation (9), yields a single fourth-order envelope equation for  $A$  as

$$\partial_Z^4 A - 8(\partial_X^2 + \partial_Y^2)\partial_Z^2 A + 16(\partial_X^2 - \partial_Y^2)^2 A + \alpha\partial_Z^2 A + i\tilde{\sigma}\partial_Z(|A|^2 A) = 0. \quad (11)$$

This novel envelope equation is one of the main results in this Letter.

It remains to relate the initial conditions for  $\Psi$  with those for the envelope equation (11). By collecting the  $\psi_0, \psi_1$  and  $\psi_2$  solutions from the above analysis and projecting the resulting perturbation-series solution (6) onto the eigenfunctions and generalized eigenfunctions, we find the dominant terms of  $\Psi$  are given by

$$\Psi \approx \epsilon^{\frac{3}{2}}(A\phi^{01} + \epsilon B\phi^{02} + \epsilon C\phi^{11} + \epsilon^2 D\phi^{21}), \quad (12)$$

where

$$C = -i(A_Z + 2A_X + 2A_Y), \quad (13)$$

$$D = -A_{ZZ} - 2A_{ZX} - 2A_{ZY} - \frac{\alpha}{2}A + 4iB_X - 4iB_Y. \quad (14)$$

Thus, from initial envelope functions  $A, B, C, D$  of the eigenfunctions and generalized eigenfunctions in  $\Psi$ , we can obtain initial conditions for  $A, A_Z, A_{ZZ}$  and  $A_{ZZZ}$  from (10), (13) and (14).

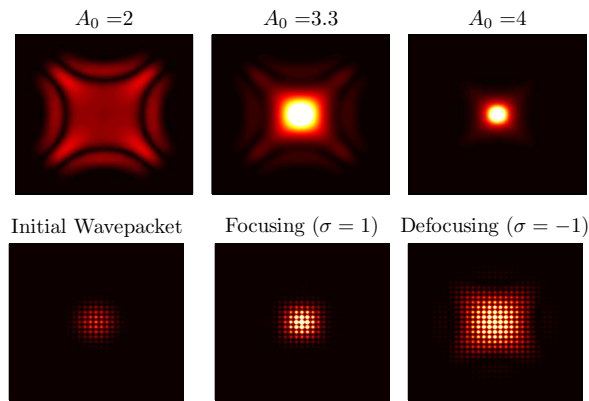


FIG. 3: Nonlinear dynamics of wave packets below phase transition. Upper row: envelope solutions in (11) at  $Z \approx 2$  for three values of  $A_0$  in (15). Lower row: solutions of the full equation (1) for the initial wavepacket with  $A_0 = 6$  (left) at later distances under focusing (middle) and defocusing (right) nonlinearities.

Direct simulations show strong agreement between the envelope dynamics in (11) and those corresponding wave packets in the full equation (1). For this letter we take the initial conditions

$$A = A_0 e^{-(X^2+Y^2)}, A_Z = A_{ZZ} = 0, \partial_Z^3 A = -i\tilde{\sigma}|A|^2 A \quad (15)$$

in the envelope equation, or the equivalent initial conditions based on (12) for simulations of the full equation (1). For the constants we take  $V_0^2 = 6$ ,  $\epsilon = 0.1$ , and  $\eta = 0$  or 1 (at or below phase transition respectively). Then we find  $\alpha = 12\eta$ , and  $\tilde{\sigma} \approx 7.3\sigma$ .

In the linear equation at the phase transition point, i.e.,  $\alpha = \tilde{\sigma} = 0$ , equation (11) has the general solution

$$A = A_1(X - 2Z, Y - 2Z) + A_2(X - 2Z, Y + 2Z) + A_3(X + 2Z, Y - 2Z) + A_4(X + 2Z, Y + 2Z) \quad (16)$$

for arbitrary  $A_n$  functions. In general this corresponds to

an expanding square wave front propagating with speeds  $\pm 2$  in both  $X$  and  $Y$  directions, which we term pyramid diffraction. This pattern is illustrated in Fig. 1 for both the envelope and full equations. Notice that the wave fronts are flat on all four sides.

In the linear equation but below the phase transition point ( $\alpha = 12$ ,  $\tilde{\sigma} = 0$ ), the pyramid diffraction is qualitatively similar to that in Fig. 1, with wave fronts expanding roughly like a square. But the wave fronts are no longer flat. In addition, the core develops an ‘x’ shape. An example is shown in Fig. 2, where diffractions in both the envelope and full equations are displayed.

In the presence of nonlinearity ( $\tilde{\sigma} \approx 7.3\sigma$ ) and below phase transition, the wave packet diffracts away if its initial amplitude is below a certain threshold value. This nonlinear diffraction is also pyramid-like, closely resembling the linear pyramid diffraction in Fig. 2. An example is displayed in Fig. 3 (upper left panel). However, if the initial amplitude is above this threshold, the envelope solution blows up to infinity in finite distance. For example, with the initial condition (15), the envelope solution in (11) blows up when  $A_0 > 3.2$ . These blowup solutions are displayed in Fig. 3 (upper middle and right panels). Remarkably, this blowup is independent of the sign of the nonlinearity, a fact which is clear from the envelope equation (11), since a sign change in  $\tilde{\sigma}$  can be accounted for by taking the complex conjugate of this equation. In the full equation (1), we have confirmed that similar growth occurs for both signs of the nonlinearity as well. For instance, evolution of a wavepacket (corresponding to  $A_0 = 6$ ) under focusing and defocusing nonlinearities are displayed in Fig. 3 (lower row). In both cases solutions rise to very high amplitudes as the envelope equation predicts.

In summary, we have analyzed nonlinear dynamics of wave packets in two-dimensional  $\mathcal{PT}$ -symmetric lattices near the phase-transition point. In the linear regime, pyramid diffraction is demonstrated. In the nonlinear regime, wave blowup is obtained for both focusing and defocusing nonlinearities.

This work is supported in part by AFOSR.

- 
- [1] C. Bender and S. Boettcher, “Real spectra in non-Hermitian Hamiltonians having  $\mathcal{PT}$  symmetry,” *Phys. Rev. Lett.* **80**, 5243–5246 (1998).
- [2] A. Ruschhaupt, F. Delgado and J. G. Muga, “Physical realization of  $\mathcal{PT}$ -symmetric potential scattering in a planar slab waveguide”, *J. Phys. A* **38**, L171-L176 (2005).
- [3] R. El-Ganainy, K. G. Makris, D. N. Christodoulides and Z. H. Musslimani, “Theory of coupled optical  $\mathcal{PT}$ -symmetric structures,” *Opt. Lett.* **32**, 2632–2634 (2007).
- [4] A. Guo, G. J. Salamo, D. Duchesne, R. Morandotti, M. Volatier-Ravat, V. Aimez, G. A. Siviloglou and D. N. Christodoulides, “Observation of  $\mathcal{PT}$ -Symmetry Breaking in Complex Optical Potentials,” *Phys. Rev. Lett.* **103**, 093902 (2009).
- [5] C. E. Rueter, K. G. Makris, R. El-Ganainy, D. N. Christodoulides, M. Segev and D. Kip, “Observation of parity-time symmetry in optics,” *Nature Physics* **6**, 192–195 (2010).
- [6] A. Regensburger, C. Bersch, M.A. Miri, G. Onishchukov, D.N. Christodoulides and U. Peschel, “Paritytime synthetic photonic lattices”, *Nature* **488**, 167-171 (2012).
- [7] R. Driben and B.A. Malomed, “Stability of solitons in parity-time-symmetric couplers”, *Opt. Lett.* **36**, 4323 (2011).
- [8] I.V. Barashenkov, S.V. Suchkov, A.A. Sukhorukov, S.V. Dmitriev, and Y.S. Kivshar, “Breathers in  $\mathcal{PT}$ -symmetric optical couplers”, *Phys. Rev. A* **86**, 053809 (2012).
- [9] Z. H. Musslimani, K. G. Makris, R. El-Ganainy and D. N. Christodoulides, “Optical solitons in  $\mathcal{PT}$  periodic potentials,” *Phys. Rev. Lett.* **100**, 030402 (2008).

- [10] S. Longhi, “Bloch oscillations in complex crystals with PT symmetry”, Phys. Rev. Lett. **103**, 123601 (2009).
- [11] K. G. Makris, R. El-Ganainy, D. N. Christodoulides and Z. H. Musslimani, “PT-symmetric optical lattices”, Phys. Rev. A **81**, 063807 (2010).
- [12] Z. Lin, H. Ramezani, T. Eichelkraut, T. Kottos, H. Cao and D.N. Christodoulides, “Unidirectional invisibility induced by PT-symmetric periodic structures”, Phys. Rev. Lett. **106**, 213901 (2011).
- [13] S. Nixon, L. Ge and J. Yang, “Stability analysis for solitons in PT-symmetric optical lattices,” Phys. Rev. A **85**, 023822 (2012).
- [14] S. Nixon, Y. Zhu, and J. Yang, “Nonlinear dynamics of wave packets in PT-symmetric optical lattices near the phase transition point”, Opt. Lett. **37**, 4874-4876 (2012).